# Structural Evolution and Stability of Hydrogenated Li-n (n=1-30) Clusters: A Density Functional Study

**ARTICLE** *in* THE JOURNAL OF PHYSICAL CHEMISTRY A · JUNE 2011

Impact Factor: 2.69 · DOI: 10.1021/jp202493u · Source: PubMed



**3 AUTHORS:**

Seema Gautam
Institute of Nano Science and Technology
**7** PUBLICATIONS **27** CITATIONS
SEE PROFILE

Keya Dharamvir
Panjab University
**127** PUBLICATIONS **499** CITATIONS
SEE PROFILE

Neetu Goel
Panjab University
**23** PUBLICATIONS **50** CITATIONS
SEE PROFILE

THE JOURNAL OF PHYSICAL CHEMISTRY A

ARTICLE

pubs.acs.org/JPCA

# Structural Evolution and Stability of Hydrogenated $Li_n$ ($n$ = 1−30) Clusters: A Density Functional Study

Seema Gautam,[†] Keya Dharamvir,[†] and Neetu Goel[*,‡]

[†]Department of Physics & Center of Advanced Studies in Physics and [‡]Department of Chemistry & Center of Advanced Studies in Chemistry, Panjab University, Chandigarh-160014, India

**ABSTRACT:** The structure and electronic and optical properties of hydrogenated lithium clusters $Li_nH_m$ ($n$ = 1−30, $m \leq n$) have been investigated by density functional theory (DFT). The structural optimizations are performed with the Becke 3 Lee−Yang−Parr (B3LYP) exchange-correlation functional with 6-311G++(d, p) basis set. The reliability of the method employed has been established by excellent agreement with computational and experimental data, wherever available. The turn over from two- to three-dimensional geometry in $Li_nH_m$ clusters is found to occur at size $n$ = 4 and $m$ = 3. Interestingly, a rock-salt-like face-centered cubic structure is seen in $Li_{13}H_{14}$. The sequential addition of hydrogen to small-sized Li clusters predicted regions of regular lattice in saturated hydrogenated clusters. This led us to focus on large-sized saturated clusters rather than to increase the number of hydrogen atoms monotonically. The lattice constants of $Li_9H_9$, $Li_{18}H_{18}$, $Li_{20}H_{20}$, and $Li_{30}H_{30}$ calculated at their optimized geometry are found to gradually approach the corresponding bulk values of 4.083. The sequential addition of hydrogen stabilizes the cluster, irrespective of the cluster size. A significant increase in stability is seen in the case of completely hydrogenated clusters, i.e., when the number of hydrogen atoms equals Li atoms. The enhanced stability has been interpreted in terms of various electronic and optical properties like adiabatic and vertical ionization potential, HOMO−LUMO gap, and polarizability.

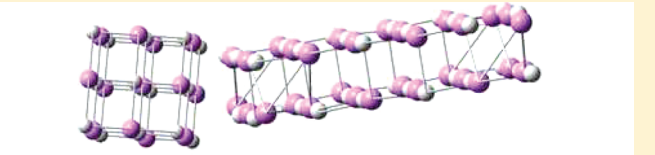

Li13H14(excess hydrogen in intersitial space and Li30H30(bulk like structure)

## INTRODUCTION

Lithium clusters are the most studied clusters in theory, and hydrogenated lithium clusters are important as models due to their low number of electrons. $Li_nH_m$ clusters appear to be the ideal prototype to study interaction of hydrogen atoms with a metal and chemisorption of hydrogen on the surface of a metal. The nature of bonding involved has been the subject of intense theoretical and experimental research. Experimental measurements of binding energy, ionization potential, and dissociation channels of hydrogenated lithium clusters are available. Theoretical calculations have provided valuable information about the geometry and other properties of the mentioned clusters. The results are explained by the hypothesis that the bonding of one hydrogen atom localizes one of the valence electrons of the Li cluster, the other electrons remaining delocalized. It has been observed that the binding of hydrogen to clusters is favored compared to that in corresponding crystals because of availability of interstitial space, lack of lattice strain energy, and lower electron density in the cluster.[1,2] The present work is based on calculations of the equilibrium structures of lithium clusters with varying hydrogen content and cluster size. Recent reports that the lithium-based metal system is a promising material for efficient hydrogen storage[3−5] have given an additional boost to their study with an aim to ascertain if LiH clusters can be efficient hydrogen storage devices. Such devices would play a crucial role in designing technologically important hydrogen storing media.

In the past two decades, mass spectroscopy and other techniques have made available experimental results on LiH clusters. Antoine et al.[2] have studied the dissociation pathway and binding energies of the $Li_nH_m^+$ clusters by using a reflectron mass spectrometer. These clusters are found to decompose into LiH and $Li_2H_2$ molecules by evaporation. The metal- insulator segregation in lithium-rich $Li_nH_m^+$ clusters has also been investigated by Antoine et al.[6] Vezin et al.[7] recorded the first vibrational and rotational spectra of $Li_2H$ and optical absorption spectra of $Li_4H$ and $Li_9H$.[8] It has been confirmed that the hydrogen atom assumes a peripheral position bridging two and three Li atoms in the planar and three-dimensional structure of $Li_4H$ and $Li_9H$, respectively. The photoionization measurements of ionization potential of $Li_nH_m$ clusters by Vezin et al.[9,10] suggest that Li clusters tend to lose metallic character as the number of hydrogen atom increases.

A variety of quantum mechanical calculations have been performed to investigate the $Li_nH_m$ cluster. Kato et al.[11] used the ab initio theory at the Hartree−Fock (HF) level to study the structure and stability of small $Li_nH_m$ ($m \leq n \leq 4$). Jena et al.[12,13] have employed the self−consistent molecular orbital method in the HF approximation to study structural and electronic properties of pure and hydrogenated Li clusters. They found that although the electronic character of Li and H in LiH is of ionic nature the electronic structure of LiH is not completely ionic. Jena et al.[14,15] also studied structural and electronic properties of

**Received:** March 16, 2011
**Revised:** May 13, 2011
**Published:** May 13, 2011

$Li_nH_m$ ($m \leq n \leq 3$) clusters and reported the difference between cluster−hydrogen and metal−hydrogen interactions. The coupled cluster computations by Shaefer et al.[16,17] show excellent agreement with available experimental data[7] for the atomization energies and ionization potentials of small $Li_n$ and $Li_nH$ ($n = 1-4$) clusters. Geometry optimizations at multireference configuration interaction (MRCI) level using large basis sets on neutral and cationic $Li_nH_m$ ($n = 1-7$, $m = 1,5$) clusters have been performed,[18,19] and high-level ab initio molecular orbital theory has also been employed[20] to calculate the geometries, vibrational frequencies, atomic charges, and binding energies of small clusters $(LiH)_n$, $(NaH)_n$, $(BeH_2)_n$, and $(MgH_2)_n$.

Since it is impractical to employ robust ab initio electronic structure methods to larger-sized clusters, recent studies on hydrogenated Li clusters are primarily based on density functional theory (DFT) which is computationally more accessible. Fuentealba et al. have conducted DFT[21,22] based studies of $Li_nH_m$ ($n \leq 4$, $m \leq 4$) clusters with the focus on static dipole polarizability and electron localization function to analyze the bonding characteristic. Bertolus et al.[23] presented a study of $Li_nH_n$ and $Li_{n+1}H_n^+$ ($n$ up to 7) and $Li_{14}H_{13}^+$ using both DFT and Model Potential, and their results have shown that Li−H is almost totally ionic. Wu and Jones[24] have presented a joint experimental/DFT study of the enthalpies of reaction for the hydrogenated Li clusters. The study of sequential hydrogen binding energies on model $Li_{18}$ clusters ($Li_{18}H_{2n+2}$, $n = 0-8$) has also been done by employing the DFT method.[25]

Up to now, though there are several measurements and theoretical researches examining the properties of $Li_nH_m$ clusters, there remain some open questions: How does hydrogenation change the properties of Li clusters? What are the preferred occupation sites of hydrogen in $Li_nH_m$ clusters? Whether a transition toward solid state can be observed in the cluster size studied here? The current work presents a comprehensive study of sequential binding of hydrogen on a Li cluster by varying hydrogen content and cluster size. Larger clusters containing dozens of Li and hydrogen atoms are probably investigated here for the first time to observe the transition to solid state.

## COMPUTATIONAL METHOD

The computations have been carried out within the DFT framework. The significant advantage of the DFT method lies in incorporating electronic correlation at a much lower cost than standard chemistry methods through an effective exchange correlation potential. The exchange correlation functional, B3LYP, is a widely used hybrid functional comprised of Becke's three-parameter exchange functional[26] and the Lee−Yang−Parr correlation functional.[27] It has been shown that B3LYP yields good results on structures and energetics of ion-covalent clusters[28] and has been successfully employed to investigate the ground state geometries and electronic structure calculations of the $Li_nH_m$ cluster.[15,21,23,25] Hadipour et al.[29] have employed the B3LYP functional with 6-311G++(2d, 2p) basis set to predict geometries, binding energies, atomic charges,[7]Li nuclear magnetic shielding, and EFG tensors of small $Li_nH_m$ ($m \leq n \leq 4$) clusters. The present work employs the B3LYP functional with 6-311G++(d, p) basis set; the double plus version in the basis set adds the diffuse function to the hydrogen and Li atom; and the p function is added for the H atom and d function for the Li atom. The calculations have been carried out using the Gaussian 03 program package.[30] It is pleasing to find that our DFT calculations reliably predict the structure evolution of large-sized $Li_nH_n$ clusters toward the bulk LiH crystal.

Numerous papers[15,18,19,21,23] have been devoted to finding global minima of small $Li_nH_m$ clusters. The present work does not attempt to find the lowest energy structure among the different isomers of $Li_nH_m$ clusters. The optimized geometry of pure $Li_n$ clusters was taken as a starting structure to build the hydrogenated lithium cluster, $Li_nH_m$. Hydrogen atoms were added one by one to the optimized $Li_n$ cluster geometry until it became completely saturated. Literature was refereed to while generating starting geometries for small-sized $Li_nH_m$ ($1 \leq n \leq 4$, $1 \leq m \leq 4$) clusters. Subsequent inputs were generated based on the optimized geometries of $Li_nH_{m-1}/Li_{n-1}H_m$. Frequency analysis was also performed over the optimized geometry at the same level of theory to check for no imaginary frequency. For the cluster $Li_nH_m$ of size ($m$, $n \leq 9$), the default self-consistent field convergence of $10^{-8}$ is used, and for a larger cluster size ($m > 9$, $n > 9$) the $10^{-6}$ convergence limit is employed. The ground state of each of the $Li_nH_m$ clusters has the lowest possible multiplicity that can be obtained for a given number of unpaired electrons. All electronic and optical calculations have been performed over optimized geometries.

## RESULTS AND DISCUSSION

**I. Structural Evolution of the $Li_nH_m$ Cluster toward the Face-Centered Cubic Bulk LiH Crystal.** The geometries of small neutral hydrogenated lithium clusters $Li_nH_m$ ($n \leq 9$, $m \leq 9$) are shown in Figure 1(a) . For LiH, the calculated bond length in the current work, i.e., 1.594 Å, is close to the experimental bond length (1.595 Å).[31] The previously theoretically reported values are 1.64,[15,21] 1.61,[18] and 1.595 Å[16] calculated by DFT,[15,21] SCF,[18] and CCSD[16] methods, respectively. Ionization extends the bond length of LiH to 2.19 Å because of Coulomb repulsion between Li and H atoms having 0.5 e charge on each. The optimized geometry of $Li_2H$ is an obtuse isosceles triangle, and the Li−Li and Li−H distances are 2.55 and 1.70 Å, respectively. These bond lengths are in agreement with those obtained by multiphoton ionization spectroscopy (2.52 and 1.71 Å)[7] and the previous calculations.[16,18,21] The geometry of the lowest energy structure of $Li_2H_2$ is a rhombus with Li−Li and Li−H bond lengths as 2.25 and 1.74 Å, respectively. These results are also in good agreement with the reported values.[19,21] It establishes that the level of theory employed in the current work strikes a fair balance between computational effort and accuracy. The initial structure of the $Li_3H$ cluster was formed by replacing one Li atom in the $Li_4$ cluster (a 60° rhombus) with a H atom, which resulted in a distorted rhombus structure after optimization, accompanied by a shortening of Li−Li bond length in the Li−H−Li subunit. A similar structure has been reported previously.[16,18,21] The optimized geometry of $Li_3H_2$ can be viewed as a deformed trapezoidal. The optimized geometry of $Li_3H_3$ is an equilateral triangle with Li atoms at the vertices and H atoms at the center of the sides, Li−Li and Li−H bond lengths being 2.75 and 1.71 Å, respectively. A similar structure has been reported in the literature.[18,25,20] The optimized geometry of $Li_4H_4$ has $T_d$ symmetry with Li−H bond length as 1.83 Å.[19−22,29] The $Li_4H_4$ cluster having eight valence electrons (sufficient to fill completely the set of degenerate one electron level) is a closed shell system. The highly symmetrical $T_d$ structure of this cluster is possible in the absence of Jahn−Teller distortion.[32] Analysis of the vibrational frequencies by Chen et al.[20] shows that with


dx.doi.org/10.1021/jp202493u |J. Phys. Chem. A 2011, 115, 6383–6389

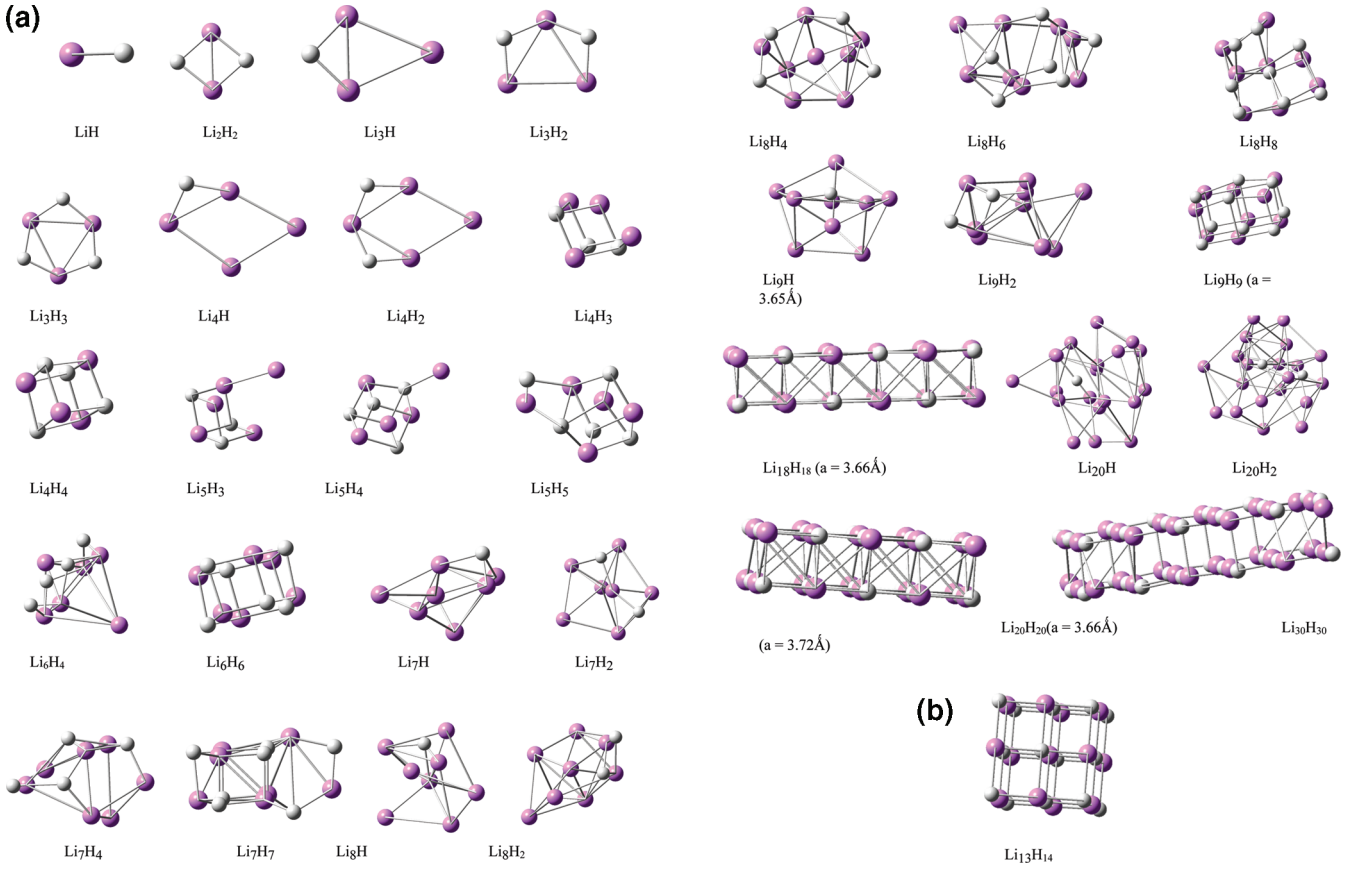


**Figure 1.** (a) Optimized geometries of neutral hydrogenated lithium $Li_nH_m$ cluster ($1 \leq n, m \geq 30$) and of $Li_9H_9$, $Li_{18}H_{18}$, $Li_{20}H_{20}$, and $Li_{30}H_{30}$ clusters with their lattice constants. (b) Optimized geometry of $Li_{13}H_{14}$.

$T_d$ symmetry $Li_4H_4$ has tetracentered bonding and is more rigid when compared to the tricentered bonded structure with $D_{4h}$ symmetry. The optimized geometry of $Li_5H_3$ is a distorted cube with F-center vacancy and also has a tail of a Li atom attached to it; the same has been reported by Koutecky et al.[19] The optimized geometry of $Li_5H_4$ is a distorted cube with a tail of a Li atom; a similar structure is found for its cationic counterpart, in contradiction to the structure reported by Bertolus et al.[23] For $Li_5H_5$ we find a chair-type structure, and $Li_6H_4$ has a caplike structure, in agreement with Koutecky et al.[19]

The optimized $Li_6H_6$ cluster has the shape of a hexagonal unit cell. The input for the geometry optimization of $Li_7H$ was generated by capping a hydrogen atom on the pentagonal bipyramid structure of $Li_7$; the distorted pentagon bipyramid with hydrogen over one of its triangular faces is obtained as the optimized structure of $Li_7H$. The optimized geometry of $Li_8H_8$ has a chair-type structure. In $Li_9H$, the H atom occupies an interstitial position between two Li atoms. For the $Li_9H_9$ cluster, nine H atoms were introduced as a cap over the triangular faces of the twisted bcc $Li_9$ cluster. The optimized structure of the $Li_9H_9$ cluster looks like an fcc unit cell with the H atoms occupying the interstitial positions between Li atoms. $Li_{13}H_{14}$ is stable with a NaCl-like fcc structure (see Figure 1b) with binding energy per atom as 2.12 eV. It seems that availability of interstitial space has made room for excess hydrogen. Most atoms in the cluster are surface atoms, so hydrogen is readily trapped. Lui et al.[33] have performed a theoretical search within the DFT framework and concluded that the interstitial position is the preferential position of the H atom in the bulk Li which has bcc structure. The position of the hydrogen atom in $Li_nH_m$ clusters studied here is in accordance with the conclusion drawn by Lui et al.[33] It indicates that the behavior of LiH clusters tends to approach the bulk behavior at small size.

This encouraged us to generate the fcc coordinates of $Li_{18}H_{18}$, $Li_{20}H_{20}$, and $Li_{30}H_{30}$ for geometry optimization. It was worthwhile to check whether the lattice constants (distance between the nearest like ions) of these cluster approach toward that of bulk lattice. Interestingly, the optimized geometries of $Li_9H_9$, $Li_{18}H_{18}$, $Li_{20}H_{20}$, and $Li_{30}H_{30}$ have the FCC structure (see Figure 1a) with an averaged value of lattice constants as 3.65, 3.66, 3.66, and 3.72 Å, respectively. The lattice constant of the bulk crystal structure of LiH is 4.084 Å.[6] It concludes that the structure of $Li_nH_m$ clusters in the nano range is the same as that of the bulk crystal structure, albeit with a relatively smaller lattice constant.

**II. Properties of $Li_nH_m$ Clusters.** *A. Binding Energy, Energy of HOMO Level, and HOMO−LUMO Gap.* Table I displays the values of binding energy per atom of $Li_nH_m$ cluster.

$$E_{BE}/(n+m) = [nE(\mathrm{Li}) + mE(\mathrm{H}) - E(\mathrm{Li}_n\mathrm{H}_m)]/(n+m)$$

Addition of hydrogen to the $Li_n$ cluster increases the binding energy, and a significant increase is observed when the number of H atoms is equal to the number of Li atoms, i.e., $Li_nH_n$ cluster. This is because of the fact that hydrogen localizes the valence electrons of the Li atom, and the saturated $Li_nH_n$ has a closed shell. There is charge transfer from the Li 2s to hydrogen 1s state. As a result, the energy of the HOMO level of the cluster gets lowered. This is reflected in the electronic behavior of the cluster


dx.doi.org/10.1021/jp202493u |J. Phys. Chem. A 2011, 115, 6383–6389

**Table I. Binding Energy Per Atom ($E_{BE}/(m+m)$), Vertical and Adiabatic Ionization Potentials (VIP/AIP), Energy of HOMO Level ($E_H$), HOMO−LUMO Gap ($E_g$), and Static Dipole Polarizability (α) of the $Li_mH_m$ Cluster at B3LYP/6-311G++(d,p)[a]**

| cluster size | $E_{BE}/(m+m)$ | VIP/AIP (EXP[e,f]) | $-E_H$ | $E_g$ | α |
|---|---|---|---|---|---|
| LiH | 1.26 (1.207[b], 1.10[d]) | 8.04/7.99(7.70[e]) | | | 28.06 |
| | | $Li_2H_m$ | | | |
| $m = 1$ | 1.20 (1.15[b], 1.38[c], 1.06[d]) | 4.79/4.16(4.10[e]) | 3.03 | 1.53 | 200.98 |
| $m = 2$ | 1.78 (2.03[c], 1.61[d]) | 8.26/7.21 | 5.71 | 5.03 | 33.41 |
| | | $Li_3H_m$ | | | |
| $m = 1$ | 1.22 (1.22[b], 1.33 [c],1.13[d]) | 5.31/5.02(4.67[e],4.74[f]) | 3.58 | 2.23 | 179.61 |
| $m = 2$ | 1.59 (1.79 [c], 1.45[d]) | 5.34/4.09(4.62[e],4.45[f]) | 3.38 | 2.46 | 129.94 |
| $m = 3$ | 1.95 (2.17 [c], 1.78[d]) | 8.68 | 6.39 | 5.78 | 49.37 |
| | | $Li_4H_m$ | | | |
| $m = 1$ | 1.12 (1.13[b], 1.22 [c]) | 4.69/4.14(4.10[e],4.17[f]) | 3.23 | 1.87 | 296.32 |
| $m = 2$ | 1.54 (1.54 [c]) | 3.62/4.68(5.00[e,f]) | 3.81 | 2.56 | 179.20 |
| $m = 3$ | 1.79 (1.95 [c], 1.63[d]) | /4.12(4.38[e,f]) | 2.94 | 2.05 | 135.55 |
| $m = 4$ | 2.04 (2.22[c]1.86[d]) | 8.45/7.99 | 6.30 | 5.68 | 65.13 |
| | | $Li_5H_m$ | | | |
| $m = 3$ | 1.73 (1.58[d]) | 5.27/4.93(4.90[e,f]) | 3.59 | 2.62 | 202.28 |
| $m = 4$ | 1.86 (1.70[d]) | 4.28, 4.21(4.33[e]) | 2.86 | 1.74 | 244.94 |
| $m = 5$ | 2.05 | 8.07/6.76 | 6.01 | 5.24 | 79.8 |
| | | $Li_6H_m$ | | | |
| $m = 4$ | 1.80 (1.65[d]) | 5.27/4.66 | 3.67 | 2.48 | 230.84 |
| $m = 6$ | 2.11 | 8.16/7.12(4.50[f]) | 6.29 | 5.47 | 91.58 |
| | | $Li_7H_m$ | | | |
| $m = 1$ | 1.12 | 4.35/4.20(4.20[e,f]) | 3.12 | 1.52 | 482.36 |
| $m = 2$ | 1.33 | 4.30/3.74(4.10[e,f]) | 3.01 | 1.52 | 462.90 |
| $m = 4$ | 1.70 | 4.25/3.64(4.18[f]) | 2.86 | 1.47 | 314.85 |
| $m = 7$ | 2.09 | 7.92/6.09 | 5.96 | 5.07 | 107.99 |
| | | $Li_8H_m$ | | | |
| $m = 1$ | 1.07 | 3.76/3.51(3.97[e],3.93[f]) | 2.62 | 1.29 | 620.55 |
| $m = 2$ | 1.32 | 4.26/4.04(4.17[f]) | 3.08 | 1.51 | 752.15 |
| $m = 4$ | 1.66 | 4.55/3.98(4.35[f]) | 3.23 | 1.86 | 365.37 |
| $m = 6$ | 1.94 | 5.20 | 3.60 | 2.53 | 242.85 |
| $m = 8$ | 2.10 | 7.49/6.03 | 5.77 | 4.83 | 121.82 |
| | | $Li_9H_m$ | | | |
| $m = 1$ | 1.08 | 3.91/3.81(4.19[e],4.18[f]) | 2.78 | 1.20 | 621.50 |
| $m = 2$ | 1.29 | 3.95/3.73(4.01[f]) | 2.77 | 1.34 | |
| $m = 9$ | 2.16 | 7.55/7.01 | 5.89 | 5.10 | 293.04 |
| | | $Li_{18}H_{18}$ | | | |
| | 2.22 | | 3.84 | 2.87 | |
| | | $Li_{20}H_m$ | | | |
| $m = 1$ | 1.10 | | 2.61 | 1.03 | |
| $m = 2$ | 1.18 | | 2.83 | 1.09 | |
| $m = 20$ | 2.12 | | 5.39 | 4.43 | |
| | | $Li_{30}H_{30}$ | | | |
| | 2.25 | | 4.40 | 4.40 | |

[a] Except, α (in au) all values are in eV. [b] Ref 16. [c] Ref 21. [d] Ref 19. [e] Ref 10. [f] Ref 9.

like reactivity and conductance. The energy of the HOMO level ($E_H$) is also listed in Table I. For example, see the value of $E_H$ for $Li_4H_n$ at $n = 1, 2, 3$, and 4 in Table I; $E_H$ of $Li_4H_4$ has significantly lowered, making it less reactive.


dx.doi.org/10.1021/jp202493u |J. Phys. Chem. A 2011, 115, 6383–6389

In accordance with the trend observed in binding energy, the HOMO−LUMO gap ($E_g$) increases as H atoms are added to the $Li_n$ cluster and particularly at the saturated level, i.e., $Li_nH_n$, shows a sudden jump. $Li_nH_m$ clusters with an even number of electrons have a higher band gap:[24] $E_g$ for $Li_4H$, $L_4H_2$, and $Li_4H_3$ is 1.87, 2.56, and 2.50 eV, respectively. The $Li_mH_n$ clusters with an even number of electrons have a closed shell and are hence more stable than the ones with an odd number of electrons.[24] However, this effect is not pronounced in larger sized clusters as the $E_g$ for $Li_{20}H_2$ (1.09) and $Li_{20}H$ (1.03) does not differ significantly.

*B. Vibrational Frequency of $Li_nH_m$ Clusters.* Frequency analysis was performed over the optimized geometry at the same level of DFT theory with 6-311G++(d, p). The vibrational frequencies thus computed followed the same trend for $Li_nH_m$ ($n = 1-4$, $m = 1-4$) as that reported in the work of Chen et al.[20] However, for higher sizes ($n = 5-9$, $m = 5-9$), there is no regular trend at the higher frequency part, as for $(LiH)_5$, $(LiH)_6$, $(LiH)_7$, $(LiH)_8$, and $(LiH)_9$ higher frequency modes are 1224, 1153, 1238, 1323, and 1272, respectively (see Table II). This is because as cluster size increases all the Li−H bond lengths are not the same and hence no general comment over the trend of vibrational frequencies with increase of cluster size can be made.

*C. Static Dipole Polarizability.* Static dipole polarizability (α) is a measure of extent of distortion of electron density, and therefore α is very sensitive to the delocalization of electrons. It is an important observable for understanding the electronic properties of clusters such as $E_g$ and Ionization Potential (IP). According to simple perturbation theory, α should be inversely correlated to the $E_g$[34] (see Table I). Values of α in the case of $Li_4H_m$ ($m = 1-4$) are decreasing, whereas their corresponding $E_g$ values are increasing with hydrogenation. This is valid for all sizes of the $Li_nH_m$ ($n = 1-9$, $m = 1-9$) cluster.

Polarizability can also be related to the cluster geometry. The increase in coordination number with cluster size leads to a decrease in polarizability.[35] As in the case of $Li_4H_m$, geometry becomes more compact as $m$ increases from 1 to 4. $Li_4H$ and $Li_4H_2$ have planar geometry, whereas $Li_4H_3$ and $Li_4H_4$ have cubic geometry (see Figure 1a).Their α value falls from 296.32 (at $m = 1$) to 65.13 (at $m = 4$), and it is true for all $Li_n$ clusters as more hydrogen atoms are added until the saturation (see Table I). Hence, we may conclude that polarizability decreases as clusters become more compact with increasing size. The above conclusion can be validated by arguing that since the polarizability per atom is a quantity related to the volume per atom of cluster the more compact structures have smaller volume and in turn have relatively few and short bonds. This leads to tighter bonding of their valence electrons. Hence their electron density is not distorted easily which means low α value. Thus, successive addition of hydrogen to $Li_n$ clusters lowers their polarizability.

The results are analyzed as a function of cluster size and composition. In the case of saturated clusters, $Li_nH_m$ ($n = m$), volume increases as the cluster size, i.e., $n$ increases (see Figure 1(a)), and as a result α increases as shown in Figure 2. The saturated hydrogenated lithium clusters $Li_nH_n$ with minimum polarizability are more stable than the metal-rich ($m < n$) cluster. This is in accordance with the minimum polarizability principal (MPP) that any system evolves toward a state of minimum polarizability.[36−38]

*D. Adiabatic and Vertical Ionization Potential.* The computed values of ionization potential (IP) are listed in Table I and compared with the experimental data[9,10] whenever possible. The vertical ionization potential (VIP) measures the energy difference between the ground state of the neutral and ionized cluster with frozen geometry of the neutral clusters, whereas adiabatic ionization potential (AIP) is a measure of the difference between the energies of the appropriate neutral form and the cationic one at their optimized geometries. It can be seen that the experimental values lie well within the predicted values of AIP and VIP.

**Table II. Frequencies ($cm^{-1}$) of the $Li_nH_m$ Cluster at 6-311G++(d, p)**

| LiH | $(LiH)_2$ | $(LiH)_3$ | $(LiH)_4$ | $(LiH)_5$ | $(LiH)_6$ | $(LiH)_7$ | $(LiH)_8$ | $(LiH)_9$ |
|---|---|---|---|---|---|---|---|---|
| 1406 | 1177 | 1234 | 1097 | 1224 | 1153 | 1238 | 1323 | 1272 |
| | 1080 | 1231 | 966 | 1208 | 1150 | 1181 | 1254 | 1243 |
| | 971 | 1214 | 965 | 1075 | 1139 | 1167 | 1239 | 1219 |
| | 888 | 1003 | 962 | 995 | 1134 | 1148 | 1178 | 1173 |
| | 601 | 944 | 944 | 962 | 1125 | 1119 | 1105 | 1091 |
| | 519 | 940 | 942 | 933 | 1009 | 1113 | 1082 | 1081 |
| | | 592 | 937 | 917 | 1006 | 1042 | 1053 | 1064 |
| | | 413 | 917 | 819 | 900 | 996 | 1008 | 1000 |
| | | 326 | 911 | 789 | 895 | 929 | 988 | 990 |
| | | 325 | 707 | 732 | 872 | 924 | 959 | 979 |
| | | 262 | 704 | 731 | 855 | 902 | 934 | 964 |
| | | 258 | 700 | 664 | 821 | 866 | 903 | 915 |
| | | | 520 | 491 | 815 | 847 | 894 | 910 |
| | | | 391 | 426 | 784 | 827 | 840 | 903 |
| | | | 390 | 408 | 718 | 795 | 809 | 893 |
| | | | 388 | 381 | 711 | 783 | 783 | 854 |
| | | | 370 | 373 | 681 | 730 | 764 | 817 |
| | | | 370 | 364 | 673 | 714 | 718 | 805 |
| | | | | 261 | 438 | 707 | 667 | 770 |
| | | | | 233 | 423 | 668 | 635 | 767 |
| | | | | 209 | 416 | 451 | 631 | 752 |
| | | | | 153 | 405 | 447 | 615 | 741 |
| | | | | | 368 | 417 | 538 | 688 |
| | | | | | 362 | 411 | 516 | 629 |
| | | | | | 326 | 378 | 479 | 613 |
| | | | | | 305 | 347 | 449 | 558 |
| | | | | | 242 | 335 | 441 | 482 |
| | | | | | 239 | 326 | 340 | 477 |
| | | | | | 182 | 292 | 410 | 461 |
| | | | | | 173 | 237 | 375 | 454 |
| | | | | | | 232 | 340 | 427 |
| | | | | | | 224 | 325 | 424 |
| | | | | | | 209 | 311 | 386 |
| | | | | | | 163 | 291 | 374 |
| | | | | | | 148 | 277 | 363 |
| | | | | | | 114 | 260 | 356 |
| | | | | | | | 231 | 344 |
| | | | | | | | 214 | 339 |
| | | | | | | | 173 | 294 |
| | | | | | | | 156 | 288 |
| | | | | | | | 145 | 287 |
| | | | | | | | 43 | 283 |
| | | | | | | | | 259 |
| | | | | | | | | 249 |
| | | | | | | | | 246 |
| | | | | | | | | 245 |
| | | | | | | | | 231 |
| | | | | | | | | 189 |

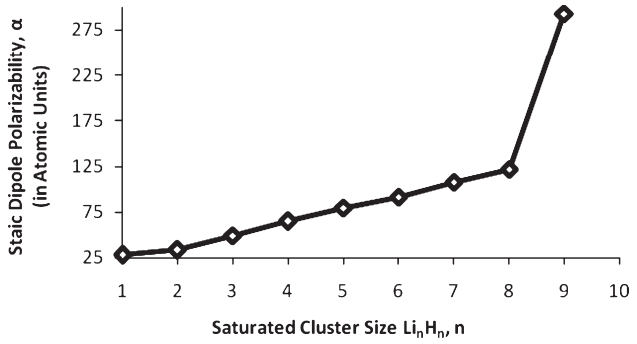


**Figure 2.** Static dipole polarizability (α) vs cluster size of the neutral saturated hydrogenated $Li_nH_m$ cluster ($1 \leq n \geq 9$, $1 \leq m \geq 9$).

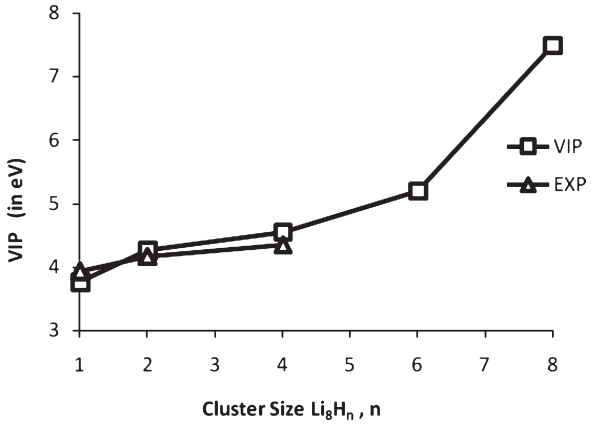


**Figure 3.** Vertical ionization potential (AIP and VIP) vs cluster size of the neutral saturated hydrogenated $Li_nH_m$ cluster ($1 \leq n \geq 9$, $1 \leq m \geq 9$).

VIP of $Li_nH_n$ clusters increases with hydrogenation (see Figure 3). Hydrogenation of lithium clusters ($Li_n$) induces the hydrogen 1s level in the respective cluster, and the valence electrons of $Li_n$ clusters are likely to transfer from the Li 2s level to the H 1s level with consequent lowering in the $E_H$ value (see Table I). When hydrogen-induced levels are sufficient enough to occupy all valence electrons of clusters, AIP and VIP show a sudden jump; i.e., IP becomes maximum for saturated lithium $Li_nH_n$ clusters. This is true for all cluster sizes. A study by Chandrakumar et al.[39] has revealed that the cube root of polarizability per atom $\alpha^{1/3}/n$ is inversely proportional to the inverse of ionization energy per atom $VIP^{-1}/n$ for both lithium $Li_n$ and sodium $Na_n$ clusters for $n = 2-10$. To explore the correlation between polarizability and ionization energy, the variation of $\alpha^{1/3}/n$ with $VIP^{-1}/n$ is investigated for $Li_8H_m$ and displayed in Figure 4

A strong correlation is observed in which $\alpha^{1/3}/n$ increases almost linearly with respect to $VIP^{-1}/n$. This correlation implies that lower ionization energy leads to a stronger binding of the valence electrons and in turn leads to a higher value of static dipole polarizability which is a measure of distortion of electron density under an external electric field.

**III. Conclusion.** The current work presents the exhaustive study of $Li_nH_m$ clusters up to a large size. The sequential addition of hydrogen to lithium metal $Li_n$ clusters has been studied by the DFT method under a B3LYP hybrid correlational functional. The accuracy of the method employed has been established by

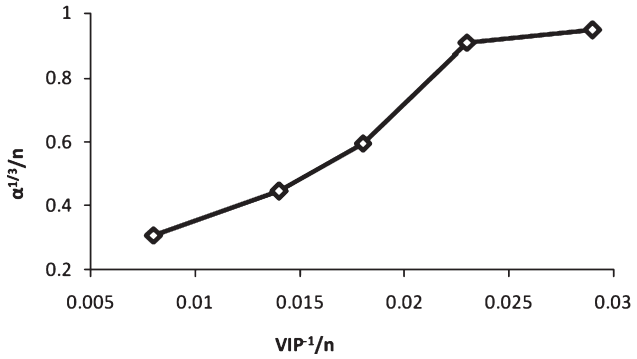


**Figure 4.** Cube root of polarizability per atom $\alpha^{1/3}/n$ vs inverse of ionization energy per atom $VIP^{-1}/n$. For $Li_8H_m$ cluster.

excellent agreement with the available literature and experimental data. The results are analyzed as a function of cluster size and composition. In particular, we follow the evolution of the properties as the composition changes from metal-rich ($m < n$) to stoichiometric ($m = n$). The sequential addition of hydrogen to small-sized Li clusters led to the conjecture that $Li_nH_m$ clusters ($n + m$ = even number) are more stable. This has been attributed to their closed shell configuration that makes it difficult to remove an electron from the doubly occupied HOMO level. There is a significant increase in the IP of the completely hydrogenated, i.e., $Li_nH_n$, clusters for all sizes. This result is consistent with the conclusion drawn by Fuentealba et al.[22] in the analysis of small-sized $Li_4H_4$ and $Li_9H$ clusters that the $Li_nH_n$ clusters have the bonds modeling an insulator. The present study demonstrates that polarizability is related to the cluster geometry, and α decreases as clusters become more compact with successive addition of hydrogen. As per the conjecture of perturbation theory, α is found to be inversely related to the HOMO−LUMO gap. The inverse correlation between the cube root of polarizability per atom $\alpha^{1/3}/n$ and the vertical ionization energy per atom $VIP^{-1}/n$ that holds good for $Li_n$ clusters[39] works for $Li_nH_m$ clusters as well. It has been established that the most stable structure of $Li_4H_4$ has $T_d$ symmetry, while $Li_6H_6$ is a hexagonal unit and the $Li_9H_9$ structure resembles fcc lattice. As the cluster is hydrogenated, it tends to form regular lattice regions with alternating Li and H ions. $Li_{18}H_{18}$, $Li_{20}H_{20}$, and $Li_{30}H_{30}$ studied by us are being reported for the first time. Interestingly, the fcc structure of the bulk LiH crystal appeared at the sizes investigated in the present work, and the lattice constant gradually approached the bulk value. In general, the metal hydrogen interaction in the $Li_nH_n$ cluster is qualitatively similar to that in the bulk LiH crystal. $Li_{13}H_{14}$ is reportedly studied here for the first time to see if it is possible to add hydrogen in excess of the metal atom. It has been found that the excess hydrogen is present at the interstitial space, indicating that it is possible to accommodate more hydrogen in the lithium hydride cluster than the corresponding bulk. However, further investigations are required to reach a firm conclusion. The vibrational frequencies computed for $Li_nH_m$ clusters showed no regular trend as cluster size increases, and therefore no general comment over the trend of vibrational frequencies with increase of cluster size can be made.

## AUTHOR INFORMATION

### Corresponding Author

*E-mail: neetu_at_chem@yahoo.com.

## ■ ACKNOWLEDGMENT

N.G. is thankful to Department of Science and Technology (DST), India, for financial support through a project grant (No.100/IFD/6358/2007-08). S.G. thanks Council of Scientific and Industrial Research (CSIR), New Delhi, for a fellowship. We are grateful to the reviewers for the constructive comments and suggestions.

## ■ REFERENCES

(1) Puska, M. J.; Nieminen, R. M. *Phys. Rev. B* **1984**, *29*, 5382.
(2) Antoine, R.; Dugourd, Ph.; Rayane, D.; Broyer, M. *J. Chem. Phys.* **1996**, *104*, 110.
(3) Chen, J.; Kuriyama, N.; Xu, Q.; Takeshita, H. T.; Sakai, T. *J. Phys. Chem. B* **2001**, *105*, 11214.
(4) Chen, P.; Xiong, Z.; Luo, J.; Lin, J.; Tan, K. L. *Nature* **2002**, *420*, 302.
(5) Pinkerton, F. E.; Meisner, G. P.; Meyer, M. S.; Balogh, M. P.; Kundrat, M. D. *J. Phys. Chem. B* **2005**, *109*, 6.
(6) Antoine, R.; Dugourd, Ph.; Rayane, D.; Benichou, E.; Broyer, M. *J. Chem. Phys.* **1997**, *107*, 2664.
(7) Vezin, B.; Dugourd, Ph.; Rayane, D.; Labasite, P.; Broyer, M. *Chem. Phys. Lett.* **1993**, *202*, 209.
(8) Vezin, B.; Dugourd, Ph.; Bordas, C.; Rayane, D.; Broyer, M.; Bonacic- Koutecky, V.; Pittner, J.; Fuchs, C.; Gaus, J.; Koutecky, J. *J. Chem. Phys.* **1995**, *102*, 2727.
(9) Vezin, B.; Rambaldi, P.; Dugourd, Ph.; Broyer, M. *J. de Phys. IV* **1994**, *4*, C4–651.
(10) Vezin, B.; Dugourd, Ph.; Rayane, D.; Labasite, P.; Chevaleyre, J.; Broyer, M. *Chem. Phys. Lett.* **1993**, *206*, 521.
(11) Kato, H.; Hirao, K.; Nishida, I.; Kimoto, K.; Akagi, K. *J. Phys. Chem.* **1981**, *85*, 3391.
(12) Rao, B. K.; Jena, P. *J. Phys. F: Met. Phys.* **1986**, *16*, 461.
(13) Rao, B. K.; Jena, P. *J. Phys. C: Solid State Phys.* **1986**, *19*, 5167.
(14) Jena, P.; Rao, B. K.; Khanna, S. N. *J. Less-Common Met.* **1991**, *172*, 387.
(15) Rao, B. K.; Khanna, S. N.; Jena, P. *Phys. Rev. B.* **1991**, *43*, 1416.
(16) Wheeler, S. E.; Sattelmeyer, K. W.; Schleyer, P. R.; Schaefer, H. F. *J. Chem. Phys.* **2004**, *120*, 4683.
(17) Wheeler, S.; Schaefer, H. F. *J. Chem. Phys.* **2005**, *122*, 204328.
(18) Bonačić- Koutecký, V.; Gaus, J.; Guest, M. F.; Češpiva, L.; Koutecký, J. *Chem. Phys. Lett.* **1993**, *206*, 528.
(19) Bonačić- Koutecký, V.; Pittner, J.; Koutecký, J. *Chem. Phys.* **1996**, *210*, 313.
(20) Chen, Y.; Huang, C.; Hu, W. *J. Phys. Chem. A* **2005**, *109*, 9627.
(21) Fuentealba, P.; Reyes, O. *J. Phys. Chem. A* **1999**, *103*, 1376.
(22) Fuentealba, P.; Savin, A. *J. Phys. Chem. A* **2001**, *105*, 11531.
(23) Bertolus, M.; Brenner, V.; Millié, P. *J. Chem. Phys.* **2001**, *115*, 4070.
(24) Wu, C. H.; Jones, R. O. *J. Chem. Phys.* **2004**, *120*, 5128.
(25) Jasien, P.; Cross, R. *J. Mol. Struct.: THEOCHEM.* **2005**, *756*, 11.
(26) Becke, A. D. *J. Chem. Phys.* **1988**, *98*, 5648.
(27) Lee, C.; Yang, W.; Parr, R. G. *Phys. Rev. B.* **1988**, *37*, 785.
(28) (a) Wang, B.; Zhai, H.; Huang, X.; Wang, L. *J. Phys. Chem. A* **2008**, *112*, 10962. (b) Ricca, A.; Bauschlicher, C. W. *Chem. Phys.* **1996**, *208*, 233.
(29) Esrafili, M. D.; Elmi, F.; Hadipour, N. L. *J. Theory Comput. Chem.* **2007**, *6*, 959.
(30) Frisch, M. J.; Truks, G. W.; Schlegelet, H. B., et al. *Gaussian 03*, revision C.3; Gaussian, Inc.: Pittsburgh, PA, 2003.
(31) Huber, K. P. Herzberg, G. *Molecular Spectra and Molecular Structure. IV. Constants of Diatomic Molecules*; Van Nostrand Reinhold Company: New York, 1979.
(32) Jahn, H. A. *Proc. R. Soc. A* **1938**, *164*, 117.
(33) Lui, Z. M.; Cui, T.; He, Z.; He, W. J.; Chen, C. B.; Zou, G. T.; Lu, G. H. *Phys. B* **2005**, *362*, 136.
(34) Vasiliev, I.; O·gÄut, S; Chelikowsky, J. R. *Phys. Rev. Lett.* **1997**, *78*, 4805.
(35) Orr, B J; Ward, J. F. *Mol. Phys.* **1971**, *20*, 513.
(36) Chattaraj, P .K; Sengupta, S. *J. Phys. Chem.* **1996**, *100*, 16126.
(37) Chattaraj, P .K; Poddar, A. *J. Phys. Chem. A* **1998**, *102*, 9944.
(38) Chattaraj., P. K; Fuentealba, P; Jaque, P; Toro-Labbe *J. Phys. Chem. A* **1999**, *103*, 9307.
(39) Chandrakumar, K. R. S.; Ghanty, T. K.; Ghosh, S. K. *J. Phys. Chem. A* **2004**, *108*, 6661.